

# ALAP-AE: As-Lite-as-Possible Auto-Encoder

Nisarg A. Shah

snisarg812@gmail.com

Gaurav Bharaj

first.last@gmail.com

AI Foundation

## Abstract

*We present a novel algorithm to reduce tensor compute required by a conditional image generation autoencoder and make it as-lite-as-possible, without sacrificing quality of photo-realistic image generation. Our method is device agnostic, and can optimize an autoencoder for a given CPU-only, GPU compute device(s) in about normal time it takes to train an autoencoder on a generic workstation. We achieve this via a two-stage novel strategy where, first, we condense the channel weights, such that, as few as possible channels are used. Then, we prune the nearly zeroed out weight activations, and fine-tune this lite autoencoder. To maintain image quality, fine-tuning is done via student-teacher training, where we reuse the condensed autoencoder as the teacher. We show performance gains for various conditional image generation tasks: segmentation mask to face images, face images to cartoonization, and finally CycleGAN-based model on horse to zebra dataset over multiple compute devices. We perform various ablation studies to justify the claims and design choices, and achieve real-time versions of various autoencoders on CPU-only devices while maintaining image quality, thus enabling at-scale deployment of such autoencoders.*

## 1. Introduction

High demand for consumer avatars, telepresence, and portrait enhancement filters such as toonification, ageing, etc. has led to an increased at-scale need of photo-realistic image generation. Such applications rely on neural image generation methods such as Generative Adversarial Networks (GANs) [10] and image-to-image style transfer methods [9, 24, 51] for supervised image and video generation via autoencoders such as U-nets, Ronneberger *et al.* [41].

Along with advancements in deep learning, availability of libraries such as PyTorch [38] and Tensorflow [1] have helped achieve photo-realistic image generation. Backends of such libraries rely on fast tensor operations, parallelized via GPU compute. However, real-time image generation via GAN-like methods has a high deployment cost due to high

GPU-based instance costs and high break-even profitability point<sup>1</sup>. Although certain edge devices are native GPUs [53] capable, they can suffer from slow inference as well as quality and resolutions deterioration of generated images. Thus, we need a solution that can quickly optimize a neural-net for a given compute device, without sacrificing image quality and leading to faster inference capabilities.

State-of-the-art literature suggests several potential approaches, such as, neural architecture design [19, 22], network architecture search (NAS) [59], neural-net compression (quantization [12], distillation [39], and pruning [12, 16]). These methods do not optimize model architectures for a given device, and target generic lightweight compute capability for cloud, workstation, or edge compute devices without having to re-design the network search space. An efficient neural-net architecture for GPU-CPU compute may not run efficiently on CPU-only compute.<sup>2</sup> Manual neural architecture design often is hard, and usually *not* device-specific. While, NAS could be employed for device specific neural-net design, such a search is expensive and requires very large amount of compute and time, while we desire a method that can optimize neural-nets on garden-variety workstations.

Typically, neural-net model compression techniques focusing primarily on image classification and detection, aren't directly usable for (conditional) GAN's autoencoder compression tasks. While compression methods for conditional GAN-based semantic segmentation exists [15], such methods lead to poor quality photo-realistic image generation. Shu *et al.* [44] propose a GAN compression evolutionary search algorithm based on channel pruning, however, the method is specifically designed for cyclic-consistency based image generation [57], and nontrivial to extend for non-cyclic consistency GANs [24, 42]. Further, Shu *et al.* [44] show that generators compressed by classifier compression methods [35] suffer performance decay compared with the original generator. Chen *et al.* [6] propose a more general

<sup>1</sup>An AWS P3 instance costs about \$3+ per hour, while a CPU-only instance costs can cost 50 times less, source: <https://aws.amazon.com/ec2/spot/pricing/>

<sup>2</sup>CPUs and GPUs intrinsically differ in hardware architecture and tensor compute wrt parallelizability, latency, and throughput per device, along with tensors transfers latency from CPU to GPU (and vice-versa).

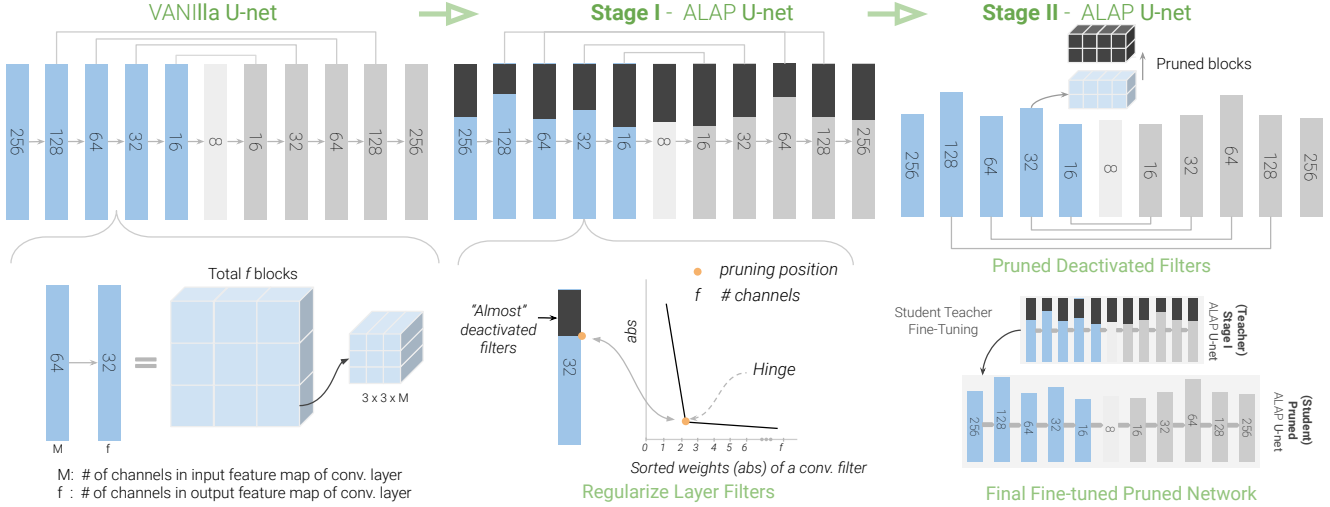


Figure 1. The proposed method for dynamic channel filter condensing and pruning GAN-based autoencoders for image generation. In Stage I, vanilla U-net autoencoder is trained with penalisation, where the weight distribution (centre-bottom) has several near-zero value channels that can be pruned. In Stage II, the pruned network is fine-tuned in student-teacher manner, using the condensed model (from Stage-I) as the teacher.

purpose GAN compression algorithm by training an efficient generator by model distillation and remove the dependency on cyclic consistency. However, their student network is handcrafted and requires significant architectural engineering for good performance.

In this work, we propose a novel strategy to optimize autoencoder’s architecture for a given compute device that makes it *as-lite-as-possible* (ALAP) wrt tensor compute required. We do this by condensing neural-net channel filter weight distribution to reduce the use of filters given a compute budget, and later, we prune the least activated filters and fine-tune using student-teacher model, where the condensed autoencoder acts as the teacher. The optimized neural-net is device agnostic and adapts the baseline architecture for the device, that is, the device’s compute capabilities, and cost budget. Further, our method also allows for a trade-off between computation complexity, and synthesized image quality, Fig 3. We summarize the novel contributions of our method as below:

1. A novel strategy to reduce compute costs via dynamic channel filter condensing and pruning GAN-based autoencoders for image generation.
2. A filter penalization loss for better filter weight distribution for easy pruning across layers, and detection of a “hinge” to get a minimum threshold for a particular filter structure to obtain ALAP version of an autoencoder.
3. Our ALAP autoencoders achieve real-time inference capabilities (with equivalent FIDs) on CPU-only, CPU-GPU compute vs. vanilla autoencoders for conditional photo-realistic image generation.

## 2. Related Works

**Conditional Image Generation** Goodfellow *et al.* [10]’s tremendous success with image generation led to several vision and graphics applications [28, 37, 49]. Conditional GANs generate images based on category labels [3], textual information [55], semantic layouts [34], or input images from various distributions [24, 25, 52]. For supervised image-to-image tasks, such as, segmentation masks to photo-realistic image generation, Isola *et al.* [24] utilizes an encoder-decoder generator, while Wang *et al.* [52] adopts a coarse-to-fine-grained generator, and multi-scale discriminator. Park *et al.* [37] propose the use of segmentation maps to predict affine transformation parameters to modulate the normalization layer’s activations for image generation. While, the emphasis of these works is to achieve better image quality, these methods require high-end (e.g. NVidia’s V100<sup>3</sup>) GPUs for fast inference. For at-scale use of such methods, lower compute instance and image inference costs is desirable.

Deep learning literature is rich in methods used to reduce the compute required for neural-nets. While most tackle non-image generation tasks, we explicitly aim to solve for conditional image generation. The methods fall under the following categories (1) Neural Architecture Design, (2) Neural Architecture Search, and (3) Neural-net Compression. Our work falls under the third category, where we tackle compute reduction by designing an algorithm that takes as input an autoencoder architecture. First, we dynamically condense the filter wight distribution by a novel filter penalization loss.

<sup>3</sup><https://www.nvidia.com/en-us/data-center/v100/>

Then, the *inactive* filters are pruned, that result in an *as-lite-as-possible* version of the input autoencoder. Our method can be employed for a wide range of devices, and latency constraints.

**Neural Architecture Design** Several deep CNNs have been proposed, AlexNet [27], VGG [13], Res-Net [45], etc. While these networks led to massive gains for vision tasks, they are fairly deep and heavy on compute; even more so in an autoencoder setting, U-net [41]. Over the year, several efficient and lightweight architectures have been proposed, Squeeze-net [20,22], Mobile-net(s) [19,43], Shuffle-net [56], Efficient-nets [48], and Ghost-net [11], etc., among several others. The emphasis of such works is to exploit a costly tensor block within the architecture, and replace it with a lightweight one, or perform tensor compute in an intelligent manner, so as to improve the performance, generally for non-image generation vision tasks. Other like Wang *et al.* [53] use depth-wise separable convolutions to reduce tensor compute for denoising applications. However, our method is a novel strategy to reduce compute for a given architecture (esp. autoencoders) in the ALAP sense, and could leverage the above mentioned architectures.

**Neural Architecture Search (NAS)** Similar to hand-designed nets, algorithms that search for efficient architectures have been devised. Such a search problem is highly nonlinear, and suffers from curse of dimensionality, and may require very large compute and time. Some works search architectures via reinforcement learning, and genetic algorithms [4,36,46] and significantly improve the performance of neural-nets. Zoph *et al.* [59] aim to search for transferable network blocks, and their performance surpasses manually designed architectures [14,47]. While Cai *et al.* [5] speeds up the exploration for better architectures via network transformation. Fu *et al.* [8] proposed a Distiller framework that adapts the search space for tasks of different properties and searches for operators types as well as channel widths. Li *et al.* [31] propose a AutoML framework that searches for channel widths for any existing generator. It is important to note that, a large amount of performance improvements can be associated to meticulously created search spaces and computationally expensive network architecture search. Compared to these works, our method optimizes accuracy and weight distribution using a penalization loss and trains in a similar time as vanilla autoencoder training. Also, our approach is orthogonal to these improvements and thus can be combined to achieve better performance at higher computational costs.

**Neural-Net Compression: Distillation, Quantization, Pruning** Network pruning is a standard method for model compression for faster inference and reduced model size.

Several works propose pruning strategies for image classification, for example, Zhu *et al.* [58] use iterative pruning techniques – Adaptive Growing and Pruning to compress models while Wen *et al.* [54] learn structured sparsity using group regularization. However, as described in [6,44], standard pruning methods that are developed for image classification tasks and do not work as well as for image generation. Wang *et al.* [50] developed a unified GAN compression framework, including model distillation, channel pruning, and quantization to address this issue. Their channel pruning method is based on [35]’s batch-norm [23] scale parameters, and measures importance among kernels of a convolutional layer. This dependence on batch-norm makes it inherently less feasible for architectures without batch-norm, while we seek a more generic approach.

Aguinaldo *et al.* [2] proposes a method to compress Radford *et al.* [40]’s DC-GAN for image generation using knowledge distillation, while Hou *et al.* [18] explores a method to generate a model with different channel size settings. While it leads to identity preserving image generation (for face images), their FIDs may deteriorate. Lin *et al.* [33] proposes a student-teacher learning method for interactive photo-realistic image generation and editing. Lin *et al.* [32] proposed an online collaborative distillation scheme to learn intermediate features of the teacher generator and discriminator for boosting the performance of the lightweight generator. Compared to these previous works, we don’t have to pre-design the student network and can condense a model for a given budget using magnitude distribution plots and “hinge” modeling, Section 3.1. However, our proposed penalisation algorithm could be used along with these student-teacher training methods for joint training as well as for device-specific optimisation.

### 3. Method

A vanilla autoencoder generator  $G$  can learn to synthesize an image  $I$  from an input segmentation map,  $S \in \{H \times W \times 3\}$ . In this pix2pix-like [24] setup, we use a U-net [41] as the backbone generator,  $G$ . The optimized generator  $G^*$  aims to be *as-lite-as-possible* ALAP, such that, the quality of generated images from both generators ( $G, G^*$ ) is nearly equivalent, while  $G^*$  can be deployed across diverse hardware – CPUs, (e)GPUs, etc., optimized for latency and image quality trade-off. The optimization condense (or regularizes) filters used on different convolution layers of an autoencoder (Stage I), and later prunes the least used filters (Stage II) and fine-tunes the pruned generator, Fig. 1.

Li *et al.* [30] and Wen *et al.* [54] propose three levels at which sparsity regularization can be realized – *fine* weight- or kernel-level, *medium* channel-level, or *coarse* layer-level sparsity regularization. *Fine* weight- or kernel-level sparsity is flexible, and generalizes well with compression rates, but requires hardware-driven acceleration to realize the gain at

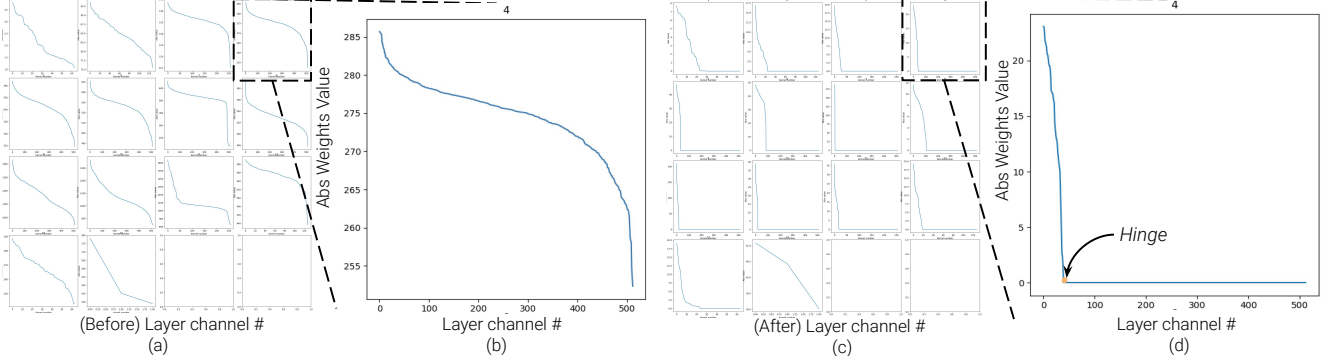


Figure 2. (a) and (c) shows the weight distribution of Unet-64’s layers after training, without and with ALAP penalisation respectively. Whereas, (b) and (d) shows the zoomed in version of there corresponding *fourth* layer. Due to effect of ALAP penalisation, as shown in (d), hinge for pruning *fourth* layer could be easily located. X-axis indicates the channel number in the layer, while Y-axis indicates the absolute value of weights of corresponding channel

inference time. While, *coarse* layer-level sparsification does not require extra hardware or software to reduce compute, it’s more rigid as the whole layer needs to be removed. Its more effectiveness when there are several layers in the CNN, unlike our generator models.

Comparatively, *medium* channel-level sparsity provides a better trade-off between flexibility and ease of deployment. This pruning method can be applied on any neural-net with convolutional layers, and generates a *sparser* and easily deployable version of the original model. Channel-level sparsity requires pruning all the adjacent connections associated with a particular channel, and makes it challenging to apply it directly on a pre-trained model due to generally non-existent zero weight channels (inactivated weights) in the neural-net, see Fig. 2 (a). To alleviate the problem of non-existent zero weight channels for sparsity regularization, we enforce a penalization loss in the training objective. Specifically, we introduce a loss function that operates on absolute value of filter weights and systematically pushes the filter weights towards zero during training.

Unlike methods like Liu *et al.* [35], that regularize on an added scaling factors after convolution or on adjacent scaling factor of normalization layer, our method operates directly on the layer’s weights. We observe that using extra scaling factors adds computational burden. Moreover, without normalization in-between, scaling factors are not a good measure for channel importance, as both CNNs and scaling parameters are linear transformations. For instance, same result could be obtained by amplifying scale parameters and correspondingly reducing the magnitude of weights of that channel. Normalization specific methods also increase the complexity of the approach when dealing with new methods with pre-activation structures and cross-connecting layers like ResNets [13], and DenseNets [21]. Further, methods designed with batch-norm (or normalisation layers in general) becomes unusable when working with newer normalisation

free architectures. Our loss function directly operates on magnitude of weights of channels, and can work with such newer architectures.<sup>4</sup>

### 3.1. Stage I - Channel Weight Regularisation

Recent channel pruning methods, like Lin *et al.* [33], utilize kernel magnitude as the criterion for relative importance across filters. On the other hand, when we train a network, a per channel importance factor  $\gamma$  is introduced, that is equivalent to magnitude of the weights of the corresponding channels. We then train the network weights and optimize the importance factor with the objective to condense the weights to be as few channels as possible. This training objective for the  $i^{th}$  layer is given by:

$$L_i = \sum_{j=0}^n f(j) * ||W_{i,j}||_1 \quad (1)$$

Where,  $n$  is layer number in the network,  $j$  the channel number of the convolutional filter, and  $W_{i,j}$  the filter weight of the  $i^{th}$  layer and  $j^{th}$  sorted channel. We tried three different channel regularisation strategies with  $j \in (0, n)$ :

- *Uniform* feature channel regularisation,  $f(j) = 1.0$
- *Linear* feature channel regularisation,  $f(j) = j$
- *Exponential* feature channel regularisation,  $f(j) = e^{0.01j}$

Various types of  $f(x)$  used as a multiplier in Eq. 1, affect the penalization that incurs by activating (i.e. having non-zero weight magnitudes) more channels. For example, in

<sup>4</sup>A layer indicates convolutional layer in the deep neural network, where a collection of channels make a single layer. For instance, if there is a  $3 \times 3$  convolutional layer, with the input feature map of shape  $H \times W \times M$  and output feature map of shape  $H \times W \times N$ , there would be total  $N$  channels each with shape  $3 \times 3 \times M$ .



Segmentation Mask	Ground Truth	Vanilla Unet-16	Vanilla Unet-32	Vanilla Unet-64	ALAP Unet-64 High reg.	ALAP Unet-64 Low reg.
CPU (FPS) ↑		70	25.9	7.3	25.2	16.4
GPU (FPS) ↑		200	168	25.9	156	131
FID ↓		74.5	58.7	47.3	48.6	37.9
Params (M) ↓		2.62	10.46	41.83	3.74	9.5

Figure 3. (Left to Right) We take several Vanilla Unet variants as baseline for conditional-GAN based Image generation (Unet-64, Unet-32, Unet-16), and create ALAP versions of the Unet-64 network for high and low regularization setting. Note: While better image generation methods exist, our emphasis is to maintain image quality vs. the baselines autoencoders.

case of *linear* feature channel regularisation compared to *uniform* feature channel regularisation, as more channels are added, the penalization increases linearly, and forces the model to condense the weights to first few channels. We

observe that due to tiny increase in value of exponential feature channel regularisation for smaller channel indices, the model compression ratio achieved was least. In our experiments, we observe linear  $f(x)$  as the standard strategy

based on trade-off perceptual image quality scores and run-time improvements, and uniform  $f(x)$  also as perform well for the tasks such as cartoonization.

### 3.2. Stage I - Layer Device Performance Regularisation

GPU devices exploit benefits of tensor compute parallelism in convolution layers and process relatively large number of weight channels. CPU devices, however, carry out these operations sequentially and don't benefit from GPU-accelerated convolutional tensor compute speeds. Depending on the type of device and their memory allocation, relative speed of convolution operation across different spatial resolutions and feature map sizes differs considerably. For example, a `convolution(kernel=3, stride=2)` at  $8 \times 8$  resolution with 512 input and output channels require 7.179 milliseconds (ms) on CPU and 1.132 ms on GPU. However, same convolution at  $16 \times 16$  resolution takes 21.12 ms ( $3 \times$  cost) and 1.840 ms ( $1.6 \times$  cost) on CPU and GPU, respectively. Similarly, for a `convolution(kernel=3, stride=2)` at  $128 \times 128$  resolution with input channel 1, if the number of output channels are increased from 32 to 128, the run-time for CPU gets quadrupled ( $4 \times$  cost) while that for GPU it remains nearly same. Based on this insight, we make the neural-net optimization device specific.

For model deployment, the compute devices are usually fixed, thus we propose run-time layer level (which depend on the device) channel regularisation strategy. We calculate the run-time for each layer across a particular device and use it as a multiplicative factor  $l(i)$  for that layer, to calculate total penalization. Also, our method allows device agnostic, or multiply-accumulate (MAC) operations based, layer level channel regularisation. To this end, we calculate the multiplicative factor of each layer based on corresponding MAC operations of that particular layer. The general formula for calculating total penalisation is given by:

$$L_{\text{PENAL}} = \sum_{i=0}^n l(i) * L_i \quad (2)$$

The objective function for a traditional minimax optimization problem [10] for a GAN is  $\min_G \max_D L_{\text{GAN}}$ , where:

$$L_{\text{GAN}} = \mathbb{E}_{y \in \mathcal{Y}} [\log(D(y))] + \mathbb{E}_{x \in \mathcal{X}} [\log(1 - D(G(x)))] \quad (3)$$

Here,  $\mathcal{X}$  corresponds to random noise distribution, while  $\mathcal{Y}$  corresponds to real image distribution. Similar to pix2pix [24], we use l1 loss (between ground-truth and generated images), for supervised training in our experiments. Based on Eqs. 2 and 3, the final training objective is given by  $\min_G \max_D L_{\text{GAN}}^{\text{ALAP}}$ , where:

$$L_{\text{GAN}}^{\text{ALAP}} = L_{\text{GAN}} + L_{\text{I1}} + L_{\text{PENAL}} \quad (4)$$

### 3.3. Stage II - Pruning and Distillation

After Stage-I training based on Equation 4, we obtain a model with a considerable amount of inactivated (near zero weight) channels. Due to penalization loss, this distinction between near zero and important channels is easily identifiable. The inclination point that shows the threshold between these two types of channels is identified as the "hinge". Figure 2 shows an example resulting weight distribution plot. Here, we sort channels of a layer in a Unet-64 model by magnitude (importance factor), and the hinge is identified at  $50^{\text{th}}$  channel for this particular layer. This way, we do not require to take an arbitrary guess or a global threshold [35] on the number of channels to be pruned, making it as-lite-as-possible for that trained model. After identifying the "hinge", channels below the hinge are pruned. Along with pruning these channels, we also remove corresponding incoming and outgoing connections and weights across all layers, and obtain a compact network with fewer parameters, run-time memory, and less compute operations.

This hinge-based pruning has a minimal effect on the perceptual quality of generated images, that can also be compensated by fine-tuning the pruned network via a student-teacher method where the Stage-I trained model acts as the teacher model. Also, it was observed that, 'almost' deactivated filters, as described Fig. 1 acts as noisy channels, thus when pruned, generate images with higher perceptual quality without any further training. Furthermore, in several cases, like the over-parameterized or low weight penalization models discussed in the subsequent section, we also find that the fine-tuned pruned network can even reach far-higher perceptual scores than the vanilla network. After this stage, we finally obtain optimized ALAP generator  $G^*$ .

## 4. Experiments

**Setup** We evaluate and ablated our method on CelebA-HQ dataset [29] that contains 30,000 high-quality face images (resized to  $256 \times 256$ ) and corresponding pixel-level segmentation mask annotations. We evaluate images generated by our optimized  $G^*$  using perceptual quality score – FID [17], memory consumption, run-times, and quantitative comparisons. We conduct experiments to translate semantic segmentation mask to face images using pix2pix [24] to compare different methods. The paired dataset is divided into about 23,500 training images, 4,000 validation images, and about 2,500 test images. To verify the efficacy of our algorithm across different autoencoders, we follow the settings in pix2pix and use U-net [41] and ResNet as generators. Like [6, 24], we use PatchGANs, that uses  $70 \times 70$  image patches instead of whole images. During optimization of the networks, the objective value is divided by two while optimizing the discriminator. The networks are trained for 200 epochs using Adam [26], and learning rate of  $1e^{-4}$ .



We use U-net [24] termed as Unet-64, where number of channels is 64 and that gets doubled after every strided convolution with an upper limit of 512. We also evaluate our approach on an *overly-parametrized* Unet-192 to observe its advantages to reduce over-fitting. We also trained Unet-32 and Unet-16 to compare the pruned variants of Unet-64 in an equi-parametric setting. Since the discriminator does not affect inference time, the student and teacher discriminator structure was kept the same. We analyze the performance of different autoencoders – Unet and ResNet, and compare their respective vanilla versions and optimized models using our proposed method. We further show application of ALAP – AE on CycleGAN for horse-to-zebra dataset, and on pix2pix to cartoonize the faces to verify the generalizability of our algorithm across different tasks and comparison with state-of-art methods available. We use MAC-based layer level regularisation and linear  $f(j)$ , Eq. 1, feature channel regularisation for experiments unless otherwise specified.

## 4.1. Results

**Qualitative Results** Fig. 3 shows additional results of several variants on U-net [41] architectures for conditional image generation. While satisfactory results are achieved for vanilla generator (Unet-64), it requires significant parameters as well as compute resources. Although, *miniature* Unet variants (Unet-16 and Unet-32) have fewer MACs (FLOPs), memory consumption, and parameters, their generated images look austere and blurry with repeated patches; thus making them look fake. While images generated by our proposed condensed generators look sharper and more realistic, at a low inference times. Here, it is important to note, that primary objective of *high-reg* version of ALAP is to develop more compressed model with equivalent perceptual scores, compared to it’s vanilla variant, whereas, in *low-reg* versions, higher perceptual quality is preferred over compression metrics. *High* and *low* indicates the amount of penalisation in the overall loss function.

**Quantitative Evaluation** Fig. 3 also shows statistics with different autoencoders. While the vanilla Unet-64 achieves satisfactory performance, it’s generator’s considerable number of parameters and long run-time prevent its applicability for cost-dependent real-time applications. The *miniature* Unet model has far fewer parameters, where we remove half (Unet-32) and three-fourth (Unet-16) of it’s filters. These generators, trained from scratch, suffer severe degradation in FID scores with no equivalent improvements in run-time.

Our algorithm was able to distribute the weights in each layer, such that, not only was it able to achieve better FIDs compared to corresponding vanilla models, but also hinge-based pruning had a minimal effect on FID scores. After student-teacher training of the model, Section 3.3, we are

able to recover from pruning artifacts and the resulting model improved FIDs by 17%. Along with, other efficiency parameters like run-time(FPS), parameters and memory also improve significantly.

**Latency reduction** We measure the latency speed-up on both CPU device (Intel Xeon CPU E5-2686) and low-cost GPU (NVidia K80), mentioned in the statistics portion of Fig. 3. Inference time for ALAP-Unet generators is consistently at  $3.5\times$  wall time speed-up on Xeon CPU and  $1.63\times$  speed-up on a NVIDIA K80 GPU with better FID scores. Interestingly, the ALAP-Unet-64 high-reg variant achieves a real-time inference on CPU device that makes it feasible for cost-effectively deployment.

## 4.2. Ablation

**Application over other AE** In the above experiments, performance of the proposed method was illustrated on a U-net autoencoder for conditional image generation (from a segmentation maps). In order to demonstrate the generalizability of our proposed method across conditional generators, we additionally apply it on ResNet, which is more complex than a U-net due to its cross-connections. In our experiments, we keep the number of channels in the first convolution layer to 128, that double after every strided convolution. We call this setup ResNet-128, while all other hyper-parameters and discriminator network are kept the same as those described in the previous experiments.

Here, we compare ALAP-ResNet with vanilla ResNet-128 model. The vanilla ResNet-128 model has 54M parameters and takes 45.47(MB) of memory but has an FID score of 47.3. Using student-teacher training (Sec 3.3), the pruned network in Stage-II learns information from the non-pruned condensed model (Stage I). Due to the inherent regularisation effect of penalization loss, the generated images look better than the vanilla version of the model. The ALAP-ResNet model achieves comparable FID performance as the vanilla ResNet network, but, with fewer parameters; demonstrating the proposed algorithm’s generality.

**Overparametrization and Regularisation effect** On quantitative part of Fig. 4, we can observe that, with Unet-192 and ALAP-Unet-192, typically there’s a  $6\times$  reduction in the number of parameters, and the weight-induced pruned network achieves a lower FID score compared to the original model. Unet-192 has an FID score of 65.3, which is 30% poorer compared to its smaller variant Unet-64’s FID of 47.3. These results are produced due to over-fitting of the Unet-192 model on the training dataset. Interestingly, our penalization algorithm solves the over-fitting problem to an extent by achieving FID improvements of 30% with  $5\times$  and  $3.2\times$  improvements on run-time over CPU and GPU, respectively. We hypothesize this is due to the regularization effect

Segmentation Mask	Ground Truth	Vanilla ResNet-128	ALAP - ResNet-128	Vanilla Unet-192	ALAP - Unet-192
CPU (FPS) ↑		0.15	0.63	0.45	2.5
GPU (FPS) ↑		3.43	6.1	7.8	25
FID ↓		52.2	49.7	65.26	42.8
Params (Million) ↓		54	4.9	376	61.5

Figure 4. (Left to Right) We take baseline conditional-GAN based AE’s (Unet-192, ResNet), and create ALAP versions of these AEs.

Segmentation Mask	Ground Truth	Aguinaldo et al. 2019	Wang et al. 2020	ALAP - Unet-64 (high reg.)
CPU (FPS) ↑		25.9	20.3	25.2
GPU (FPS) ↑		168	142	156
FID ↓		55.9	52.6	48.6
Parameters (Million) ↓		10.46	6.72	3.74

Figure 5. (Left to Right) Comparison with recent state-of-art Distillation and Pruning methods. (Segmentation Mask, Ground Truth, Aguinaldo *et al.* [2], Wang *et al.* [50], ALAP-Unet-64(high reg.)

of the penalisation algorithm on channels that condenses the features in each layer, and make redundant channel weights zero.

**Channel Weight and Layer Device Regularisation** Our channel weight regularisation method supports several multiplicative functions like Uniform, Linear, and Exponential. Uniform and Exponential factors are used in low reg form.

The quantitative predictions for different channel weight multiplicative factors discussed in Sec. 3.1 are shown in Fig. 6. Kindly, refer supplementary material for qualitative results. We also tested the results for device agnostic layer level regularisation discussed in Sec 3.2 in Fig. 7. Here, specific improvements over inference time of model could be observed for the model optimised for that corresponding device i.e. CPU and GPU.



Ground Truth	Linear Pen. (High reg.)	Uniform Penalization	Exponential Penalization	Linear Penal. (Low reg.)
CPU (FPS) ↑	25.2	22.5	21.9	16.4
GPU (FPS) ↑	156	149	144	131
FID ↓	48.6	45.61	44.46	37.9

Figure 6. (Left to Right) We create the ALAP versions of Unet-64 variant with different Channel weight regularisation. ( *Linear*(high-reg.), *Uniform*, *Exponential*, *Linear*(low-reg.) feature channel regularisation)

Segmentation Mask	Ground Truth	Vanilla Unet-64	ALAP - Unet-64- CPU	ALAP - Unet-64- GPU	ALAP - Unet-64- MAC
CPU (FPS) ↑		7.3	28.6	26.1	25.2
GPU (FPS) ↑		96	161	169	156
FID ↓		47.3	51.48	51.61	48.6
Parameters (Million) ↓		41.83	3.04	3.18	3.74

Figure 7. (Left to Right) Comparison of (high-reg) Unet-64 variants condensed for particular type of Device e.g. CPU, GPU and general (MAC) (Segmentation Map, Ground truth, Unet-64, ALAP-Unet-64-[CPU, GPU, MAC])

**Comparison with State-of-the-Art Compression Methods for Conditional Image generation.** Aguinaldo *et al.* [2] uses model distillation to train a slim student generator from the corresponding bigger teacher network. Since conditional image-generation is challenging, we used Unet-64 as the teacher network and Unet-32, i.e., half slimmed channels for every layer as the student network and train using the distillation method. We observe from Fig. 5, that the image generated from this approach, though with slightly improved FID scores, generate blurry results. We also imple-

mented Wang *et al.* [50] for the vanilla Unet-64 and obtain improved results in terms of perceptual quality (FID), parameter reduction, and memory usage compared with [2]. However, images generated from [50] have several artifacts such as, random color patterns, illuminations and thus, quality of generated images look inferior to our methods, while both networks have similar sizes and runtime, see Figure 5.

**Comparison of ALAP on Cartoonisation task.** Experiments are conducted on CelebA-HQ dataset and cartoon

	ResNet	Shu et al. [44]	Wang et al. [50]	ALAP-ResNet (high reg.)
FID	148.81	139.88	120	133
Flops (Giga)	52.90	12.16	12.05	8.21
Memory (MB)	43.51	10.02	9.04	4.83

Table 1. Comparison with the state-of-the-art GAN compression methods [44] and [50] on CycleGAN Zebra-to-horse compression task.

Face Images	Ground Truth	UNet-64	ALAP-UNet-64 Linear (low reg.)	ALAP-UNet-64 Uniform(Stage-1)	ALAP-UNet-64 Uniform(Stage-2)
FID ↓		29.20	27.52	25.65	24.31
Parameters (Million) ↓		41 M	18.5 M	41 M	7.8 M
Memory (MB) ↓		160 MB	96 MB	160 MB	30 MB
CPU (FPS) ↑		7.4	8.2	7.4	11.6
GPU (FPS) ↑		96	107	96	119

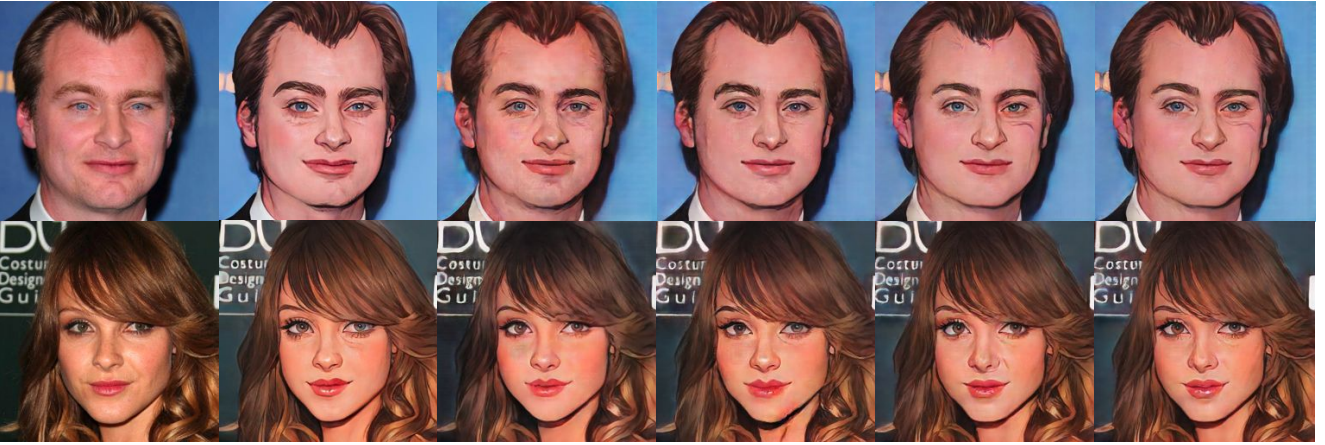


Figure 8. Pix2pix compression results: Face cartoonization (Left to Right) Face Image, Cartoonized face, results by UNet-64, ALAP-UNet-64 Linear (low reg.), ALAP-UNet-64 Uniform (Stage-1), and ALAP-UNet-64 Uniform (Stage-2) respectively. FIDs, Parameters(in M), model size (in MB), CPU run-time and GPU run-time of each method are annotated above images.

images for paired training, where cartoon images were generated using the animegan2 repo<sup>5</sup>. We test our method on two different channel weight regularisation approaches, i.e., Uniform and Linear, and the weighing of penalization is controlled to get balanced improvements over both FID scores and compression metrics. Both training and testing are done at  $256 \times 256$  resolution. The qualitative and quantitative results of the cartoon-style transfer, together with model statistics (FLOPs and model sizes), are shown in Fig. 8. We also show results after only stage-1 training to quantify student-teacher’s effect on our approach. We note that results that the naive student-teacher approach has a minimal effect on FID scores. Exploring improved student-teacher methods for training is orthogonal to our work and could be leveraged for additional improvements. We observe from the results that uniform channel weight regularisation performs better compared to its linear version. We also observe that uniform weight regularisation performs slightly better when

fine-scale features are less critical in the generation process. ALAP-UNet performs remarkably well compared to UNet, with a 20% improvement on FID scores and a 6x reduction in the number of parameters. These results validate our ALAP approach superiority compared to the models trained with the conventional approach in terms of perceptual quality and model parameters.

**Comparison of ALAP on CycleGAN application.** In the above experiments, we demonstrate the performance of the proposed ALAP method on paired image-to-image translation employing pix2pix. In order to illustrate generalization ability of the proposed algorithm, we further apply it on unpaired image-to-to image translation, that is more complex than paired translation, using CycleGAN [57]. We evaluate our ALAP-CycleGAN on the horse-to-zebra dataset. We used the ResNet model used in [57] for our generator for a fair comparison with the recent state-of-art methods like GAN-sliming [31]. We note that CycleGAN has two genera-

<sup>5</sup><https://github.com/bryandlee/animegan2-pytorch>



Source Image	UNet-64	ResNet	Shu et al.	Wang et al.	ALAP-ResNet
FID ↓	138	71.87	96	88	62.72
Flops (Giga) ↓	6.03 G	52.90 G	12.51 G	11.36 G	10.9 G
Memory (MB) ↓	160 MB	43.51 MB	10.19 MB	8.7 MB	7.42 MB

Figure 9. CycleGAN compression results: horse-to-zebra task. (Left to Right) Source Image, Style transfer results by UNet-64, ResNet CycleGAN, CEC [44], GAN-Sliming [50] and ALAP-ResNet respectively. FIDs, FLOPs (in G) and model size (in MB) of each method are annotated above images.

tors to translate from domain A to B and B to A, we apply penalization loss on the single generator. Following [44, 50], we utilize the GFLOPs and model size (MB) to measure the generator’s efficiency and measure FID between source style-transfer results and target-style images to measure the effectiveness of ResNet based generator quantitatively. On horse-to-zebra task, ALAP-ResNet achieves  $5.9\times$  reduction in model size compared to baseline with 30% FID improvement. The visual and quantitative results comparison are collectively displayed in Fig. 9. We also observe that our algorithm was able to achieve significant improvement of 28% in FID scores compared to Wang *et al.* [50] along with improved results over compression matrices. For the task, of style transfer from zebra-to-horse, using high-reg. version of ALAP-ResNet we were able to achieve a 33% reduction in the number of flops and  $11\times$  reduction in memory usage with improvements over perceptual quality metrics.

## 5. Limitations and Conclusion

We present ALAP-AE, a tensor compute reduction method that optimizes neural autoencoders for photo-realistic conditional image generation, for any compute device, achieving near real-time inference capabilities on CPU-only and GPU devices. Our methods show significant improvement over state-of-the-art methods, wrt run-time and perceptual quality for photo-realistic image generation on CPU devices for various conditional image generation tasks. We verify our approach by creating optimized models for CPU as well as GPU devices, and show our methods efficacy for run-time performance and image quality.

While, several limitations exist: Our method does not preserve the complete identity attributes when the network is optimized vs. vanilla versions of the autoencoders, however we note that such a solution is task specific. Along with, our method requires manually picking hinges during stage-II pruning. Finally, we note that various tasks performed well with under different penalization strategy that were manually decided. In the future, we’d like to explore improvements for these limitations, via better perceptual losses during training to achieve lower FID scores, introduce identity preserving losses using methods like [7], and propose automated hinge selection via clustering and curve curvature modeling, etc. to assist in iterative training procedure.

## References

- [1] Martín Abadi, Paul Barham, Jianmin Chen, Zhifeng Chen, Andy Davis, Jeffrey Dean, Matthieu Devin, Sanjay Ghemawat, Geoffrey Irving, Michael Isard, et al. Tensorflow: A system for large-scale machine learning. In *12th {USENIX} symposium on operating systems design and implementation ({OSDI} 16)*, pages 265–283, 2016. 1
- [2] Angeline Aguineldo, Ping-Yeh Chiang, Alex Gain, Ameya Patil, Koltan Pearson, and Soheil Feizi. Compressing gans using knowledge distillation. *arXiv preprint arXiv:1902.00159*, 2019. 3, 8, 9
- [3] Andrew Brock, Jeff Donahue, and Karen Simonyan. Large scale gan training for high fidelity natural image synthesis. *arXiv preprint arXiv:1809.11096*, 2018. 2
- [4] Andrew Brock, Theodore Lim, James M Ritchie, and Nick Weston. Smash: one-shot model architecture search through hypernetworks. *arXiv preprint arXiv:1708.05344*, 2017. 3



- [5] Han Cai, Tianyao Chen, Weinan Zhang, Yong Yu, and Jun Wang. Reinforcement learning for architecture search by network transformation. *arXiv preprint arXiv:1707.04873*, 4, 2017. 3
- [6] Hanting Chen, Yunhe Wang, Han Shu, Changyuan Wen, Chunjing Xu, Boxin Shi, Chao Xu, and Chang Xu. Distilling portable generative adversarial networks for image translation. In *Proceedings of the AAAI Conference on Artificial Intelligence*, 2020. 1, 3, 6
- [7] Jiankang Deng, Jia Guo, Niannan Xue, and Stefanos Zafeiriou. Arcface: Additive angular margin loss for deep face recognition. In *Proceedings of the IEEE/CVF Conference on Computer Vision and Pattern Recognition*, pages 4690–4699, 2019. 11
- [8] Yonggan Fu, Wuyang Chen, Haotao Wang, Haoran Li, Yingyan Lin, and Zhangyang Wang. Autogan-distiller: Searching to compress generative adversarial networks. *arXiv preprint arXiv:2006.08198*, 2020. 3
- [9] Leon A Gatys, Alexander S Ecker, and Matthias Bethge. Image style transfer using convolutional neural networks. In *Proceedings of the IEEE conference on computer vision and pattern recognition*, pages 2414–2423, 2016. 1
- [10] Ian Goodfellow, Jean Pouget-Abadie, Mehdi Mirza, Bing Xu, David Warde-Farley, Sherjil Ozair, Aaron Courville, and Yoshua Bengio. Generative adversarial nets. *Advances in neural information processing systems*, 27, 2014. 1, 2, 6
- [11] Kai Han, Yunhe Wang, Qi Tian, Jianyuan Guo, Chunjing Xu, and Chang Xu. Ghostnet: More features from cheap operations. In *Proceedings of the IEEE/CVF Conference on Computer Vision and Pattern Recognition*, pages 1580–1589, 2020. 3
- [12] Song Han, Huizi Mao, and William J Dally. Deep compression: Compressing deep neural networks with pruning, trained quantization and huffman coding. *arXiv preprint arXiv:1510.00149*, 2015. 1
- [13] Kaiming He, Xiangyu Zhang, Shaoqing Ren, and Jian Sun. Deep residual learning for image recognition. In *Proceedings of the IEEE conference on computer vision and pattern recognition*, pages 770–778, 2016. 3, 4
- [14] Kaiming He, Xiangyu Zhang, Shaoqing Ren, and Jian Sun. Identity mappings in deep residual networks. In *European conference on computer vision*, pages 630–645. Springer, 2016. 3
- [15] Yang He, Ping Liu, Ziwei Wang, Zhilan Hu, and Yi Yang. Filter pruning via geometric median for deep convolutional neural networks acceleration. In *Proceedings of the IEEE/CVF Conference on Computer Vision and Pattern Recognition*, pages 4340–4349, 2019. 1
- [16] Yihui He, Xiangyu Zhang, and Jian Sun. Channel pruning for accelerating very deep neural networks. In *Proceedings of the IEEE international conference on computer vision*, pages 1389–1397, 2017. 1
- [17] Martin Heusel, Hubert Ramsauer, Thomas Unterthiner, Bernhard Nessler, and Sepp Hochreiter. Gans trained by a two time-scale update rule converge to a local nash equilibrium. *Advances in neural information processing systems*, 30, 2017. 6
- [18] Liang Hou, Zehuan Yuan, Lei Huang, Huawei Shen, Xueqi Cheng, and Changhu Wang. Slimmable generative adversarial networks. *arXiv preprint arXiv:2012.05660*, 2020. 3
- [19] Andrew G Howard, Menglong Zhu, Bo Chen, Dmitry Kalenichenko, Weijun Wang, Tobias Weyand, Marco Andreetto, and Hartwig Adam. Mobilenets: Efficient convolutional neural networks for mobile vision applications. *arXiv preprint arXiv:1704.04861*, 2017. 1, 3
- [20] Jie Hu, Li Shen, and Gang Sun. Squeeze-and-excitation networks. In *Proceedings of the IEEE conference on computer vision and pattern recognition*, pages 7132–7141, 2018. 3
- [21] Gao Huang, Zhuang Liu, Laurens Van Der Maaten, and Kilian Q Weinberger. Densely connected convolutional networks. In *Proceedings of the IEEE conference on computer vision and pattern recognition*, pages 4700–4708, 2017. 4
- [22] Forrest N Iandola, Song Han, Matthew W Moskewicz, Khalid Ashraf, William J Dally, and Kurt Keutzer. Squeezenet: Alexnet-level accuracy with 50x fewer parameters and 0.5 mb model size. *arXiv preprint arXiv:1602.07360*, 2016. 1, 3
- [23] Sergey Ioffe and Christian Szegedy. Batch normalization: Accelerating deep network training by reducing internal covariate shift. In *International conference on machine learning*, pages 448–456. PMLR, 2015. 3
- [24] Phillip Isola, Jun-Yan Zhu, Tinghui Zhou, and Alexei A Efros. Image-to-image translation with conditional adversarial networks. In *Proceedings of the IEEE conference on computer vision and pattern recognition*, pages 1125–1134, 2017. 1, 2, 3, 6, 7
- [25] Tero Karras, Samuli Laine, Miika Aittala, Janne Hellsten, Jaakko Lehtinen, and Timo Aila. Analyzing and improving the image quality of stylegan. In *Proceedings of the IEEE/CVF Conference on Computer Vision and Pattern Recognition*, pages 8110–8119, 2020. 2
- [26] Diederik P Kingma and Jimmy Ba. Adam: A method for stochastic optimization. *arXiv preprint arXiv:1412.6980*, 2014. 6
- [27] Alex Krizhevsky, Ilya Sutskever, and Geoffrey E Hinton. ImageNet classification with deep convolutional neural networks. *Communications of the ACM*, 60(6):84–90, 2017. 3
- [28] Christian Ledig, Lucas Theis, Ferenc Huszár, Jose Caballero, Andrew Cunningham, Alejandro Acosta, Andrew Aitken, Alykhan Tejani, Johannes Totz, Zehan Wang, et al. Photo-realistic single image super-resolution using a generative adversarial network. In *Proceedings of the IEEE conference on computer vision and pattern recognition*, pages 4681–4690, 2017. 2
- [29] Cheng-Han Lee, Ziwei Liu, Lingyun Wu, and Ping Luo. Maskgan: Towards diverse and interactive facial image manipulation. In *IEEE Conference on Computer Vision and Pattern Recognition (CVPR)*, 2020. 6
- [30] Hao Li, Asim Kadav, Igor Durdanovic, Hanan Samet, and Hans Peter Graf. Pruning filters for efficient convnets. *arXiv preprint arXiv:1608.08710*, 2016. 3
- [31] Muyang Li, Ji Lin, Yaoyao Ding, Zhijian Liu, Jun-Yan Zhu, and Song Han. Gan compression: Efficient architectures for interactive conditional gans. In *Proceedings of the IEEE/CVF conference on computer vision and pattern recognition*, pages 5284–5294, 2020. 3, 10

- [32] Shaojie Li, Jie Wu, Xuefeng Xiao, Fei Chao, Xudong Mao, and Rongrong Ji. Revisiting discriminator in gan compression: A generator-discriminator cooperative compression scheme. *Advances in Neural Information Processing Systems*, 34, 2021. 3
- [33] Ji Lin, Richard Zhang, Frieder Ganz, Song Han, and Jun-Yan Zhu. Anycost gans for interactive image synthesis and editing. In *Proceedings of the IEEE/CVF Conference on Computer Vision and Pattern Recognition*, pages 14986–14996, 2021. 3, 4
- [34] Xihui Liu, Guojun Yin, Jing Shao, Xiaogang Wang, and Hongsheng Li. Learning to predict layout-to-image conditional convolutions for semantic image synthesis. *arXiv preprint arXiv:1910.06809*, 2019. 2
- [35] Zhuang Liu, Jianguo Li, Zhiqiang Shen, Gao Huang, Shoumeng Yan, and Changshui Zhang. Learning efficient convolutional networks through network slimming. In *Proceedings of the IEEE international conference on computer vision*, pages 2736–2744, 2017. 1, 3, 4, 6
- [36] Risto Miikkilainen, Jason Liang, Elliot Meyerson, Aditya Rawal, Daniel Fink, Olivier Francon, Bala Raju, Hormoz Shahrzad, Arshak Navruzyan, Nigel Duffy, et al. Evolving deep neural networks. In *Artificial intelligence in the age of neural networks and brain computing*, pages 293–312. Elsevier, 2019. 3
- [37] Taesung Park, Ming-Yu Liu, Ting-Chun Wang, and Jun-Yan Zhu. Semantic image synthesis with spatially-adaptive normalization. In *Proceedings of the IEEE/CVF Conference on Computer Vision and Pattern Recognition*, pages 2337–2346, 2019. 2
- [38] Adam Paszke, Sam Gross, Francisco Massa, Adam Lerer, James Bradbury, Gregory Chanan, Trevor Killeen, Zeming Lin, Natalia Gimelshein, Luca Antiga, et al. Pytorch: An imperative style, high-performance deep learning library. *Advances in neural information processing systems*, 32:8026–8037, 2019. 1
- [39] Antonio Polino, Razvan Pascanu, and Dan Alistarh. Model compression via distillation and quantization. *arXiv preprint arXiv:1802.05668*, 2018. 1
- [40] Alec Radford, Luke Metz, and Soumith Chintala. Unsupervised representation learning with deep convolutional generative adversarial networks. *arXiv preprint arXiv:1511.06434*, 2015. 3
- [41] Olaf Ronneberger, Philipp Fischer, and Thomas Brox. U-net: Convolutional networks for biomedical image segmentation. In *International Conference on Medical image computing and computer-assisted intervention*, pages 234–241. Springer, 2015. 1, 3, 6, 7
- [42] Arsiom Sanakoyeu, Dmytro Kotovenko, Sabine Lang, and Bjorn Ommer. A style-aware content loss for real-time hd style transfer. In *proceedings of the European conference on computer vision (ECCV)*, pages 698–714, 2018. 1
- [43] Mark Sandler, Andrew Howard, Menglong Zhu, Andrey Zhmoginov, and Liang-Chieh Chen. Mobilenetv2: Inverted residuals and linear bottlenecks. In *Proceedings of the IEEE conference on computer vision and pattern recognition*, pages 4510–4520, 2018. 3
- [44] Han Shu, Yunhe Wang, Xu Jia, Kai Han, Hanting Chen, Chunjing Xu, Qi Tian, and Chang Xu. Co-evolutionary compression for unpaired image translation. In *Proceedings of the IEEE/CVF International Conference on Computer Vision*, pages 3235–3244, 2019. 1, 3, 10, 11
- [45] Karen Simonyan and Andrew Zisserman. Very deep convolutional networks for large-scale image recognition. *arXiv preprint arXiv:1409.1556*, 2014. 3
- [46] Kenneth O Stanley and Risto Miikkilainen. Evolving neural networks through augmenting topologies. *Evolutionary computation*, 10(2):99–127, 2002. 3
- [47] Christian Szegedy, Wei Liu, Yangqing Jia, Pierre Sermanet, Scott Reed, Dragomir Anguelov, Dumitru Erhan, Vincent Vanhoucke, and Andrew Rabinovich. Going deeper with convolutions. In *Proceedings of the IEEE conference on computer vision and pattern recognition*, pages 1–9, 2015. 3
- [48] Mingxing Tan and Quoc Le. Efficientnet: Rethinking model scaling for convolutional neural networks. In *International Conference on Machine Learning*, pages 6105–6114. PMLR, 2019. 3
- [49] Ayush Tewari, Mohamed Elgharib, Gaurav Bharaj, Florian Bernard, Hans-Peter Seidel, Patrick Pérez, Michael Zöllhofer, and Christian Theobalt. Stylerig: Rigging stylegan for 3d control over portrait images, cvpr 2020. In *IEEE Conference on Computer Vision and Pattern Recognition (CVPR)*. IEEE, june 2020. 2
- [50] Haotao Wang, Shupeng Gui, Haichuan Yang, Ji Liu, and Zhangyang Wang. Gan slimming: All-in-one gan compression by a unified optimization framework. In *European Conference on Computer Vision*, pages 54–73. Springer, 2020. 3, 8, 9, 10, 11
- [51] Ting-Chun Wang, Ming-Yu Liu, Jun-Yan Zhu, Guilin Liu, Andrew Tao, Jan Kautz, and Bryan Catanzaro. Video-to-video synthesis. *arXiv preprint arXiv:1808.06601*, 2018. 1
- [52] Ting-Chun Wang, Ming-Yu Liu, Jun-Yan Zhu, Andrew Tao, Jan Kautz, and Bryan Catanzaro. High-resolution image synthesis and semantic manipulation with conditional gans. In *Proceedings of the IEEE conference on computer vision and pattern recognition*, pages 8798–8807, 2018. 2
- [53] Yuzhi Wang, Haibin Huang, Qin Xu, Jiaming Liu, Yiqun Liu, and Jue Wang. Practical deep raw image denoising on mobile devices. In *European Conference on Computer Vision*, pages 1–16. Springer, 2020. 1, 3
- [54] Wei Wen, Chunpeng Wu, Yandan Wang, Yiran Chen, and Hai Li. Learning structured sparsity in deep neural networks. *Advances in neural information processing systems*, 29:2074–2082, 2016. 3
- [55] Han Zhang, Tao Xu, Hongsheng Li, Shaoting Zhang, Xiaogang Wang, Xiaolei Huang, and Dimitris N Metaxas. Stackgan: Text to photo-realistic image synthesis with stacked generative adversarial networks. In *Proceedings of the IEEE international conference on computer vision*, pages 5907–5915, 2017. 2
- [56] Xiangyu Zhang, Xinyu Zhou, Mengxiao Lin, and Jian Sun. Shufflenet: An extremely efficient convolutional neural network for mobile devices. In *Proceedings of the IEEE conference on computer vision and pattern recognition*, pages 6848–6856, 2018. 3

- [57] Jun-Yan Zhu, Taesung Park, Phillip Isola, and Alexei A Efros. Unpaired image-to-image translation using cycle-consistent adversarial networks. In *Proceedings of the IEEE international conference on computer vision*, pages 2223–2232, 2017. [1](#), [10](#)
- [58] Michael Zhu and Suyog Gupta. To prune, or not to prune: exploring the efficacy of pruning for model compression. *arXiv preprint arXiv:1710.01878*, 2017. [3](#)
- [59] Barret Zoph, Vijay Vasudevan, Jonathon Shlens, and Quoc V Le. Learning transferable architectures for scalable image recognition. In *Proceedings of the IEEE conference on computer vision and pattern recognition*, pages 8697–8710, 2018. [1](#), [3](#)